



Rethinking Boundary Discontinuity Problem for Oriented Object Detection

Hang Xu^{1,2*}, Xinyuan Liu^{2*}, Haonan Xu², Yike Ma², Zunjie Zhu¹, Chenggang Yan¹, Feng Dai^{2†}

¹ Hangzhou Dianzi University, Hangzhou, China

² Institute of Computing Technology, Chinese Academy of Sciences, Beijing, China

*Equal contribution †Corresponding author



CONTENTS

01

Motivation

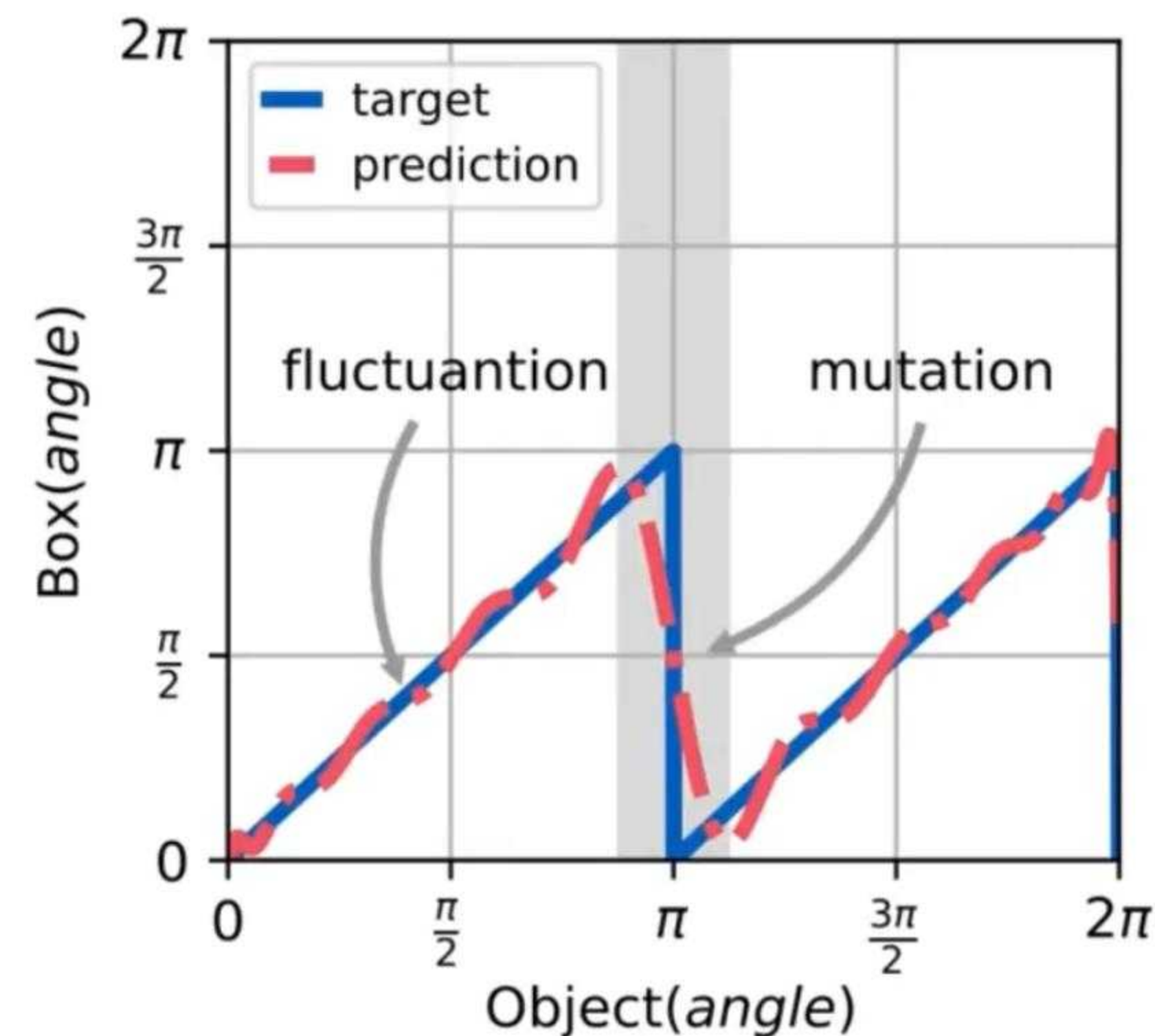
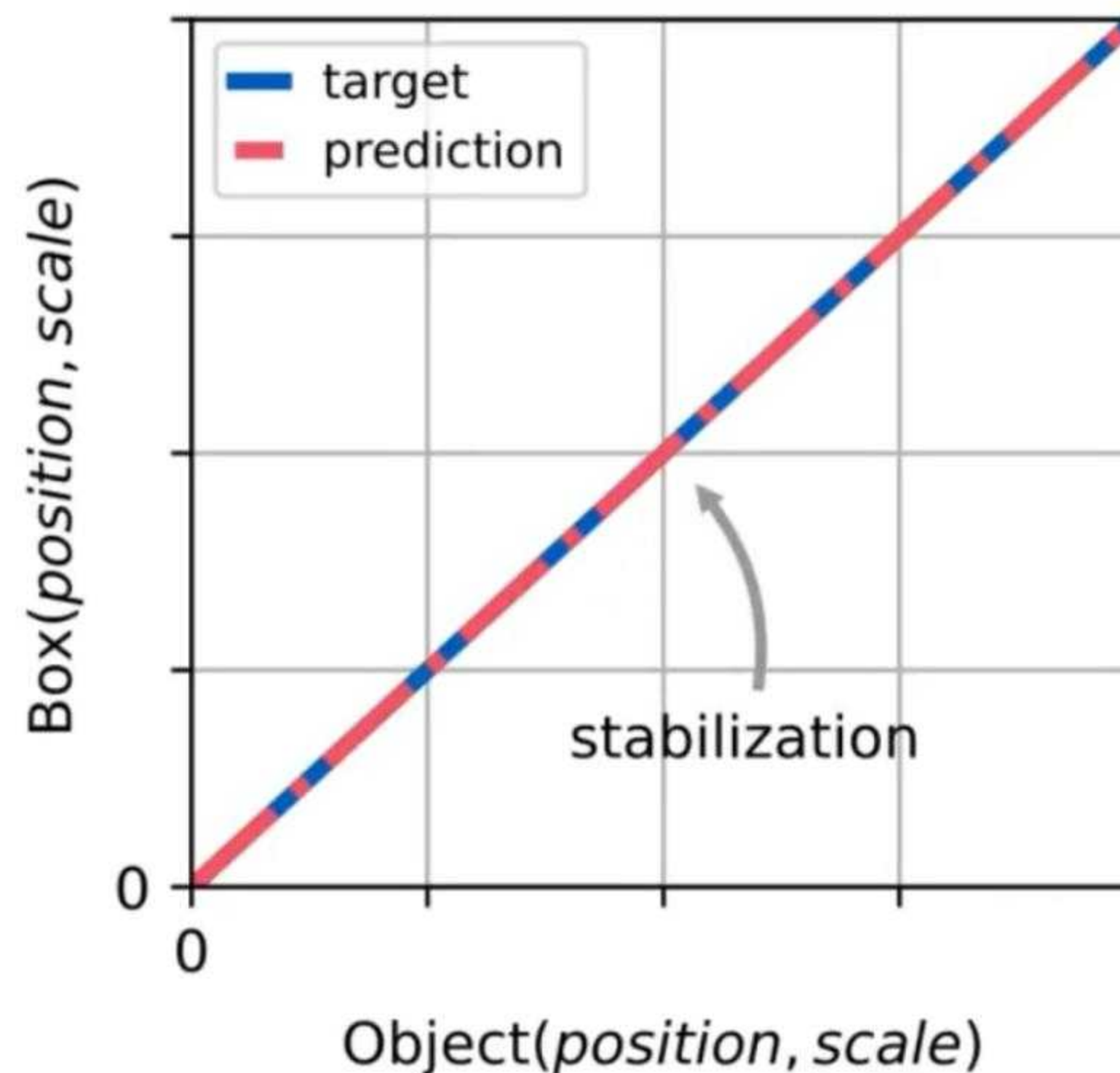
02

Method

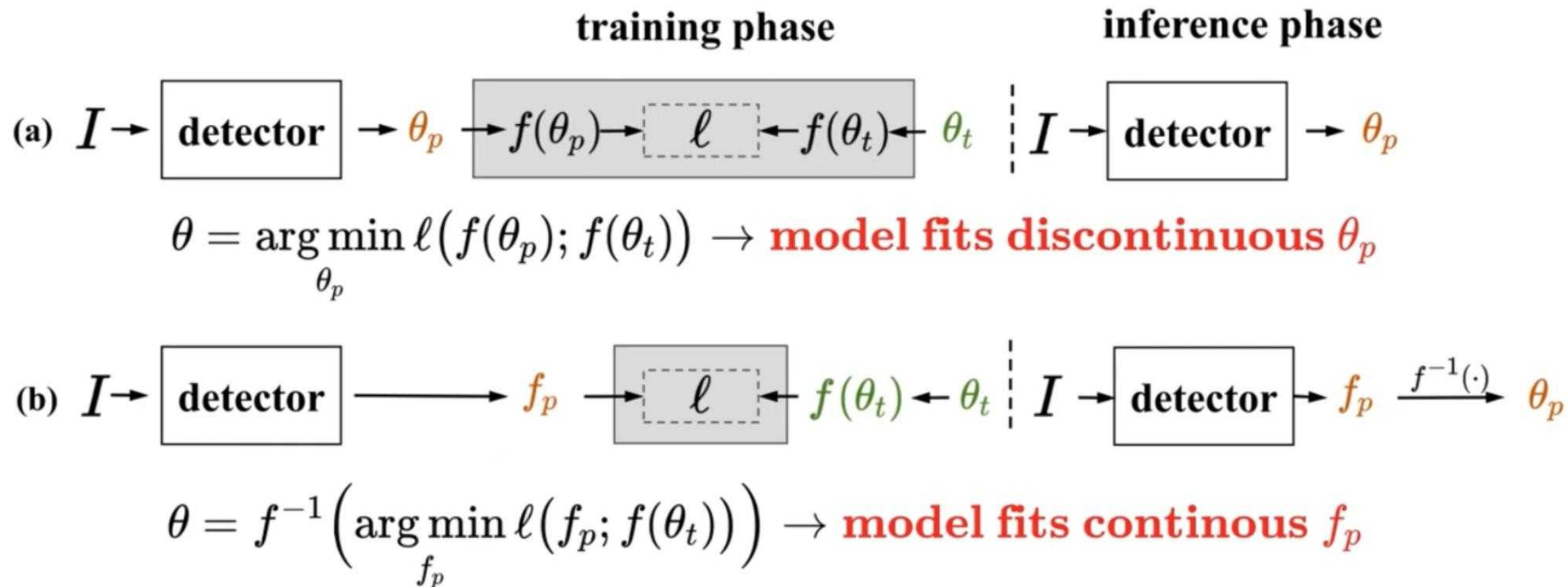
03

Experiment

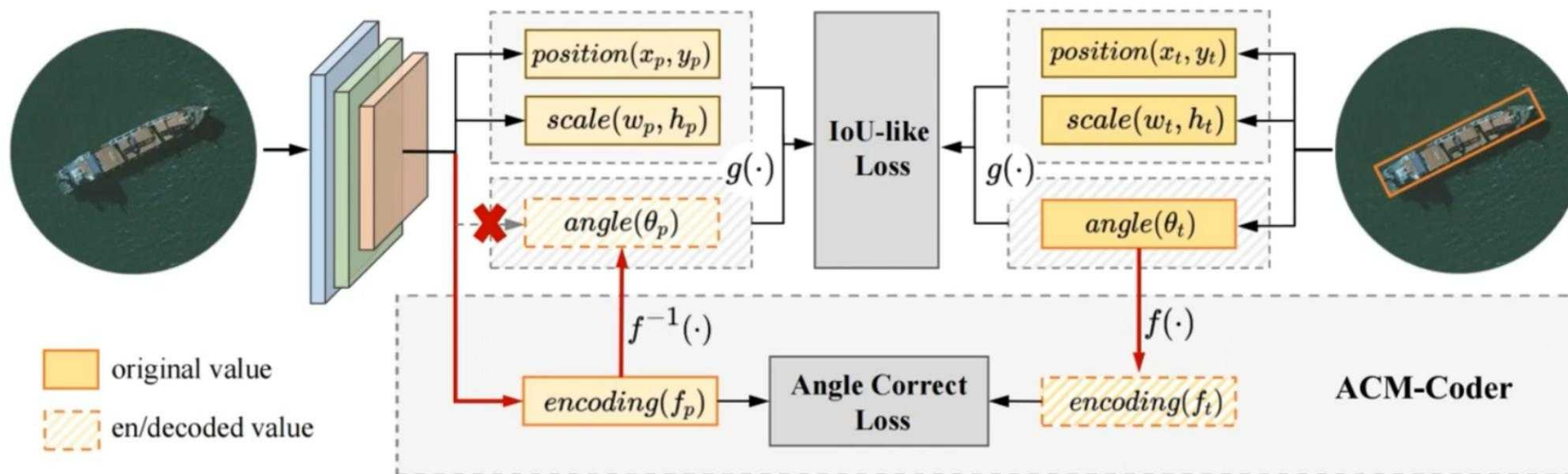
1.1 The Root of All Evil is “Box \neq Object”



1.2 The Devil is in Encoding Mode



2.1 Dual-Optimization Paradigm



2.2 ACM-Coder

- $z = f(\theta) = e^{j\omega\theta}$
- $f_{box} = e^{i\omega\theta_{box}} = e^{i\omega(\theta_{obj} \bmod \pi)} = \begin{cases} e^{i\omega\theta_{obj}}, & \theta_{obj} \in [0, \pi) \\ e^{i\omega\theta_{obj}} \cdot e^{-i\omega\pi}, & \theta_{obj} \in [\pi, 2\pi) \end{cases}$

1) When $\omega = 1$, $e^{-i\omega\pi} = -1$, then

$$f_{box} = e^{i\omega\theta_{box}} = \begin{cases} e^{i\omega\theta_{obj}}, & \theta_{obj} \in [0, \pi) \\ -e^{i\omega\theta_{obj}}, & \theta_{obj} \in [\pi, 2\pi) \end{cases} = \begin{cases} f_{obj}, & \theta_{obj} \in [0, \pi) \\ -f_{obj}, & \theta_{obj} \in [\pi, 2\pi) \end{cases} = f_{obj} \cdot \text{sign}(\pi - \theta_{obj})$$

2) When $\omega = 2$, $e^{-i\omega\pi} = 1$, then

$$f_{box} = e^{i\omega\theta_{box}} = \begin{cases} e^{i\omega\theta_{obj}}, & \theta_{obj} \in [0, \pi) \\ e^{i\omega\theta_{obj}}, & \theta_{obj} \in [\pi, 2\pi) \end{cases} = f_{obj}$$

Thus, we select $w=2$ for ACM.

3. Experiment

3.1 Comparison with the State-of-the-Art

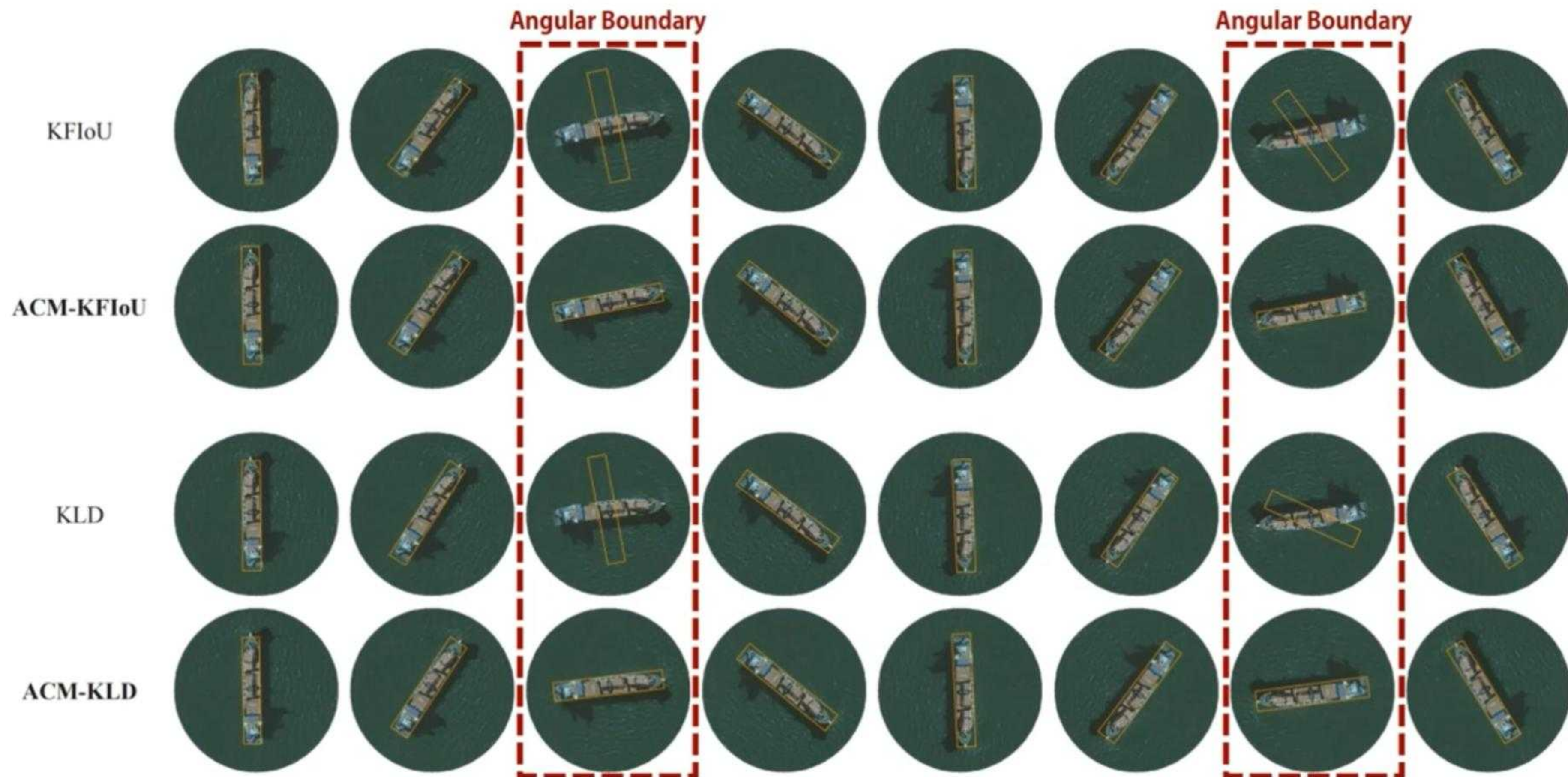
Method	MS	PL	BD	BR	GTF	SV	LV	SH	TC	BC	ST	SBF	RA	HA	SP	HC	AP ₅₀
PloU		80.90	69.70	24.10	60.20	38.30	64.40	64.80	90.90	77.20	70.40	46.50	37.10	57.10	61.90	64.00	60.50
Rol-Trans.	✓	88.64	78.52	43.44	75.92	68.81	73.68	83.59	90.74	77.27	81.46	58.39	53.54	62.83	58.93	47.67	69.56
O ² -DNet	✓	89.31	82.14	47.33	61.21	71.32	74.03	78.62	90.76	82.23	81.36	60.93	60.17	58.21	66.98	61.03	71.04
DAL	✓	88.61	79.69	46.27	70.37	65.89	76.10	78.53	90.84	79.98	78.41	58.71	62.02	69.23	71.32	60.65	71.78
P-RSDet	✓	88.58	77.83	50.44	69.29	71.10	75.79	78.66	90.88	80.10	81.71	57.92	63.03	66.30	69.77	63.13	72.30
BBAVectors	✓	88.35	79.96	50.69	62.18	78.43	78.98	87.94	90.85	83.58	84.35	54.13	60.24	65.22	64.28	55.70	72.32
DRN	✓	89.71	82.34	47.22	64.10	76.22	74.43	85.84	90.57	86.18	84.89	57.65	61.93	69.30	69.63	58.48	73.23
CFC-Net	✓	89.08	80.41	52.41	70.02	76.28	78.11	87.21	90.89	84.47	85.64	60.51	61.52	67.82	68.02	50.09	73.50
Gliding Vertex		89.64	85.00	52.26	77.34	73.01	73.14	86.82	90.74	79.02	86.81	59.55	70.91	72.94	70.86	57.32	75.02
Mask OBB	✓	89.56	85.95	54.21	72.90	76.52	74.16	85.63	89.85	83.81	86.48	54.89	69.64	73.94	69.06	63.32	75.33
CenterMap	✓	89.83	84.41	54.60	70.25	77.66	78.32	87.19	90.66	84.89	85.27	56.46	69.23	74.13	71.56	66.06	76.03
CSL	✓	90.25	85.53	54.64	75.31	70.44	73.51	77.62	90.84	86.15	86.69	69.60	68.04	73.83	71.10	68.93	76.17
R ³ Det	✓	89.80	83.77	48.11	66.77	78.76	83.27	87.84	90.82	85.38	85.51	65.67	62.68	67.53	78.56	72.62	76.47
GWD	✓	86.96	83.88	54.36	77.53	74.41	68.48	80.34	86.62	83.41	85.55	73.47	67.77	72.57	75.76	73.40	76.30
SCRDet++	✓	90.05	84.39	55.44	73.99	77.54	71.11	86.05	90.67	87.32	87.08	69.62	68.90	73.74	71.29	65.08	76.81
KFloU	✓	89.46	85.72	54.94	80.37	77.16	69.23	80.90	90.79	87.79	86.13	73.32	68.11	75.23	71.61	69.49	77.35
DCL	✓	89.26	83.60	53.54	72.76	79.04	82.56	87.31	90.67	86.59	86.98	67.49	66.88	73.29	70.56	69.99	77.37
RIDet	✓	89.31	80.77	54.07	76.38	79.81	81.99	89.13	90.72	83.58	87.22	64.42	67.56	78.08	79.17	62.07	77.62
PSC	✓	89.86	86.02	54.94	62.02	81.90	85.48	88.39	90.73	86.90	88.82	63.94	69.19	76.84	82.75	63.24	78.07
KLD	✓	88.91	85.23	53.64	81.23	78.20	76.99	84.58	89.50	86.84	86.38	71.69	68.06	75.95	72.23	75.42	78.32
CenterNet-ACM	✓	89.84	85.50	53.84	74.78	80.77	82.81	88.92	90.82	87.18	86.53	64.09	66.27	77.51	79.62	69.57	78.53
Rol-Trans.-ACM	✓	85.55	80.53	61.21	75.40	80.35	85.60	88.32	89.88	87.13	87.10	68.15	67.94	78.75	79.82	75.96	79.45

3.2 Ablation Study

Method	HRSC2016 (Ship)		UCAS-AOD (Car)		UCAS-AOD (Plane)		DOTA-v1.0	
	AP ₅₀	AP ₇₅	AP ₅₀	AP ₇₅	AP ₅₀	AP ₇₅	AP ₅₀	AP ₇₅
GWD	84.94	61.87	87.25	28.46	90.34	38.22	73.12	34.98
ACM-GWD	90.63 (+5.69)	86.71 (+24.84)	88.69 (+1.44)	29.15 (+0.69)	90.35 (+0.01)	76.00 (+37.78)	73.71 (+0.59)	41.97 (+6.99)
KLD	90.01	79.29	87.54	29.99	90.33	29.19	73.41	35.25
ACM-KLD	90.55 (+0.54)	87.45 (+8.16)	88.76 (+1.22)	30.40 (+0.41)	90.39 (+0.06)	75.65 (+46.46)	73.95 (+0.54)	42.97 (+7.72)
KFIoU	88.26	62.95	85.74	24.44	90.34	16.81	71.97	26.11
ACM-KFIoU	90.55 (+2.29)	87.77 (+24.82)	88.31 (+2.57)	34.81 (+10.37)	90.40 (+0.06)	74.48 (+57.67)	74.51 (+2.54)	40.49 (+14.38)
SkewIoU	89.39	76.43	87.73	27.59	90.34	63.64	73.62	38.01
ACM-SkewIoU	90.47 (+1.08)	88.33 (+11.09)	88.27 (+0.54)	29.13 (+1.74)	90.37 (+0.03)	75.13 (+11.49)	74.21 (+0.59)	42.83 (+4.37)

Typical IoU-like methods are improved to the same level, indicating that the primary distinction between them lies in their optimization capabilities for the angular boundary.

3.3 Visualized Results





Rethinking Boundary Discontinuity Problem for Oriented Object Detection

Hang Xu^{1,2*}, Xinyuan Liu^{2*}, Haonan Xu², Yike Ma², Zunjie Zhu¹, Chenggang Yan¹, Feng Dai^{2†}

¹ Hangzhou Dianzi University, Hangzhou, China

² Institute of Computing Technology, Chinese Academy of Sciences, Beijing, China

*Equal contribution †Corresponding author



Any questions please contact us!